# Models for Polysilane High Polymers. 1. Singlet Photophysics of Linear Permethylhexadecasilane ($Si_{16}Me_{34}$)

**Ya-Ping Sun,[1a] Yoshitaka Hamada,[1b] Li-Ming Huang,[1b] Jim Maxka,[1b] Jiunn-Shyong Hsiao,[1a] Robert West,[1b] and Josef Michl*,[1a,c]**

*Contribution from the Department of Chemistry and Biochemistry, University of Colorado, Boulder, Colorado 80309-0215, and Department of Chemistry, University of Wisconsin, Madison, Wisconsin 53706.* *Received December 27, 1991*

**Abstract:** An investigation of the UV absorption and emission properties of *n*-$Si_{16}Me_{34}$ in room- and low-temperature solutions revealed a striking similarity to the photophysical behavior of high molecular weight peralkylated polysilanes. The absorption is that expected for a statistical collection of chromophoric segments. Room-temperature emission is that expected from the lowest excitation energy conformations of approximately 16-silicon chains, presumably all-trans. Their excited states are believed to be generated by energy transfer in the polymer and by adiabatic conformational transformations in the hexadecasilane. The latter process is suppressed in 3-methylpentane glass, where many spectrally distinct conformers are observed to behave independently. Three of them dominate and have been characterized spectrally. At concentrations of $5 \times 10^{-6}$ M and higher, 3-methylpentane solutions of $Si_{16}Me_{34}$ formed dimeric or oligomeric species upon fast cooling and precipitated a microcrystalline solid upon slow cooling. These, too, have been spectrally characterized.

## Introduction

The unusual optical properties of the formally saturated polysilane high polymers, $[SiRR']_x$, have recently attracted considerable attention.[2] In room-temperature hydrocarbon solution, polysilanes with R = R' = alkyl form random coils[3] and exhibit an intense absorption band at 305-320 nm and a strong fluorescence peak at 335-345 nm. Primarily on the basis of its long-axis polarization,[4-6] this strong absorption has been assigned to a $\sigma-\sigma^*$ transition. Upon cooling below about -30 °C, the absorption and emission bands become much narrower and shift to about 350 nm, with a very small Stokes shift. It has been proposed[7] that this transformation is due to a coil-to-rod transition, but it now appears more likely that it is associated with an aggregation of long, approximately all-trans chain segments, intramolecular and/or intermolecular, depending on concentration.[8]

It has been noted[4,5,9,10] that the photophysical properties of the high-temperature solution form of the polysilanes can be understood if the polymer chain behaves as a string of fairly localized loosely coupled chromophores represented by approximately planar all-trans chain segments, separated by one or more stronger (e.g., gauche) twists. The $\sigma-\sigma^*$ excitation energy of a segment decreases rapidly as a function of its length at first and reaches a limiting value when the segment contains a dozen silicon atoms or so. After initial light absorption, the chromophores undergo fluorescence, intersystem crossing, and energy transfer from the shorter segments to longer ones, as well as photochemical transformations from both the singlet and the triplet excited states. This "conformationally determined chain segment" model for the high-temperature form of polysilanes has recently been elaborated further[11] and has received support from fluorescence quenching measurements, whose results argue against the alternative wormlike chain model.[12]

According to the segment model, the inhomogeneous broadening of the room-temperature solution spectra of polysilanes has three intramolecular causes in addition to the usual solvent effects:[9] a distribution of chain segment lengths, a distribution of deviations from exact planarity within a segment ("wormlike" chain segment behavior), and a distribution of alkyl side chain conformations. In the low-temperature form, the segment lengths are presumably almost all so large that a variation in their length has only a very small effect on the excitation energy, so that the first source of inhomogeneous broadening is much less important, the absorption band is much narrower, and the optical inhomogeneity is dominated by random disorder within the segments.[13]

In order to probe the validity of these hypotheses further, we have investigated the photophysical properties of model peralkylated linear oligosilanes of relatively short chain length ($Si_{16}Me_{34}$, $Si_{10}Me_{22}$, and $Si_6Me_{14}$). Presently, we report the results for $Si_{16}Me_{34}$ and compare them with those for high molecular weight poly(methylpropylsilane) compounds, $[SiMePr]_x$.

## Experimental Section

**Materials.** Permethylhexadecasilane $Si_{16}Me_{34}$[14] and poly(methylpropylsilane) $[SiMePr]_x$[15] were prepared by literature procedures. The molecular weight of the polymer was determined by gel permeation chromatography using a UV absorption detector and polystyrene stand-

(1) (a) The bulk of this work was performed while Y.-P.S., J.-S.H., and J.M. were still at the Center for Structure and Reactivity, Department of Chemistry, University of Texas, Austin, TX 78712. (b) University of Wisconsin. (c) University of Colorado.

(2) (a) Michl, J.; Sun, Y.-P. In *Radiation Effects on Polymeric Materials*; Reichmanis, E., O'Donnell, J. H., Frank, C. W., Eds.; ACS Symposium Series; American Chemical Society: Washington, DC, in press. (b) West, R. *J. Organomet. Chem.* **1986**, *300*, 327. (c) Miller, R. D.; Michl, J. *Chem. Rev.* **1989**, *89*, 1359.

(3) Cotts, P. M.; Miller, R. D.; Trefonas, P., III; West, R.; Fickes, G. N. *Macromolecules* **1987**, *20*, 1047.

(4) Klingensmith, K. A.; Downing, J. W.; Miller, R. D.; Michl, J. *J. Am. Chem. Soc.* **1986**, *108*, 7438.

(5) Michl, J.; Downing, J. W.; Karatsu, T.; Klingensmith, K. A.; Wallraff, G. M.; Miller, R. D. In *Inorganic and Organometallic Polymers*; Zeldin, M., Wynne, K., Allock, H., Eds.; ACS Symposium Series 360; American Chemical Society: Washington, DC, 1988; Chapter 5, p 61.

(6) (a) Harrah, L. A.; Zeigler, J. M. *Macromolecules* **1987**, *20*, 601. (b) McCrary, V. R.; Sette, F.; Chen, C. T.; Lovinger, A. J.; Robin, M. B.; Stöhr, J.; Zeigler, J. M. *J. Chem. Phys.* **1988**, *88*, 5925.

(7) Harrah, L. A.; Zeigler, J. M. *J. Polym. Sci., Polym. Lett. Ed.* **1985**, *23*, 209. Schweitzer, K. S. *J. Chem. Phys.* **1986**, *85*, 1156. Schweitzer, K. S. *J. Chem. Phys.* **1986**, *85*, 1176.

(8) Miller, R. D.; Wallraff, G. M.; Baier, M.; Cotts, P. M.; Shukla, P.; Russell, T. P.; De Schryver, F. C.; Declercq, D. Submitted for publication.

(9) Michl, J.; Downing, J. W.; Karatsu, T.; McKinley, A. J.; Poggi, G.; Wallraff, G. M.; Sooriyakumaran, R.; Miller, R. D. *Pure Appl. Chem.* **1988**, *60*, 959.

(10) (a) Johnson, G. E.; McGrane, K. M. In *Photophysics of Polymers*; Hoyle, C. E., Torkelson, J. M., Eds.; ACS Symposium Series 358; American Chemical Society: Washington, DC, 1987; p 499. (b) Kim, Y. R.; Lee, M.; Thorne, J. R. G.; Hochstrasser, R. M.; Zeigler, J. M. *Chem. Phys. Lett.* **1988**, *145*, 75. (c) Rauscher, U.; Bässler, H.; Taylor, R. *Chem. Phys. Lett.* **1989**, *162*, 127. (d) Harrah, L. A.; Zeigler, J. M. In *Photophysics of Polymers*; Hoyle, C. E., Torkelson, J. M., Eds.; ACS Symposium Series 358; American Chemical Society: Washington, DC, 1987; p 482. (e) Walsh, C.; Burland, D. M.; Miller, R. D. *Chem. Phys. Lett.* **1990**, *175*, 197.

(11) Sun, Y.-P.; Miller, R. D.; Sooriyakumaran, R.; Michl, J. *J. Inorg. Organomet. Polym.* **1991**, *1*, 3.

(12) Sun, Y.-P.; Wallraff, G. M.; Miller, R. D.; Michl, J. *J. Photochem. Photobiol. A: Chem.* **1991**, *62*, 333.

(13) Thorne, J. R. G.; Ohsako, Y.; Repinec, S. T.; Abrash, S. A.; Hochstrasser, R. M.; Zeigler, J. M. *J. Lumin.* **1990**, *45*, 295. Tilgner, A.; Pique, J. P.; Trommsdorff, H. P.; Zeigler, J. M.; Hochstrasser, R. M. ACS-APS Meeting, Washington, DC, August 1990, *Polym. Prepr.* **1990**, *31*, 244.

(14) Maxka, J.; Huang, L.-M.; West, R. *Organometallics* **1991**, *10*, 656.

(15) Miller, R. D.; Hofer, D.; McKean, D. R.; Willson, C. G.; West, R.; Trefonas, P., III In *Materials for Microlithography*; Thompson, L. F., Willson, C. G., Frechet, T. M. J., Eds.; ACS Symposium Series 266; American Chemical Society: Washington, DC, 1984; p 293.

0002-7863/92/1514-6301$03.00/0 

ards: $M_w = 7.8 \times 10^6$ and $M_n = 4.1 \times 10^6$. Anthracene (Aldrich Gold Label, 99.9%) and 9,10-diphenylanthracene (Aldrich, 99%) were used as fluorescence standards at room and low temperature, respectively. Hexane (Baker Photrex or Mallinckrodt SpectrAR) and 3-methylpentane (Phillips Pure Grade or Aldrich 99+%) were stirred for more than 24 h with concentrated sulfuric acid, fuming sulfuric acid, and concentrated sulfuric acid again, washed successively with water, a very dilute NaOH solution, and water until neutral, dried over $CaCl_2$, and fractionally distilled in the presence of sodium metal under nitrogen gas.

**Measurements.** Absorption spectra were recorded on a Cary 2300 absorption spectrophotometer. Fluorescence spectra were measured at right angle geometry on an SLM Aminco SPF-500C emission spectrophotometer equipped with a 300-W Xe lamp. For room-temperature measurements, static and flow square cells were used, always with fresh solutions. Fluorescence quantum yields obtained using a flow cell and a static cell were always in very good agreement. Unlike high molecular weight polysilanes, $Si_{16}Me_{34}$ did not photodecompose significantly even in the static cell.

All low-temperature spectroscopic measurements were carried out in an optical quartz dewar with three Suprasil windows. A 1-cm square cell was used for dilute samples and a flat 2-mm cell for concentrated samples. The latter was oriented at about 45° with respect to the exciting and the monitored beams (front surface geometry). The concentrations given refer to room-temperature conditions and contain no correction for solvent contraction.

Two kinds of glassy solutions of $Si_{16}Me_{34}$ in 3-methylpentane at 77 K, rapidly cooled and slowly cooled, were prepared. The rapid cooling was achieved by directly dipping a room-temperature solution into liquid nitrogen, and the slow cooling was accomplished by keeping the sample immediately above the surface of liquid nitrogen in an optical dewar for a period of time (usually about 30 min) at a temperature of −80 to −140 °C.

A solid film of $Si_{16}Me_{34}$ was prepared by evaporating a concentrated hexane solution of $Si_{16}Me_{34}$ on the outside surface of a quartz cell. The film was measured with liquid (room temperature) or glassy (77 K) 3-methylpentane inside the cell as background.

Fluorescence quantum yields of $Si_{16}Me_{34}$ and $[SiMePr]_x$ in room-temperature hexane solution at their corresponding absorption maxima were determined using anthracene ($\Phi_F = 0.3$)[16] as a fluorescence standard. Because of the technical difficulty of matching the experimental conditions of the standard with that of the sample in an optical dewar, for $Si_{16}Me_{34}$ in a 3-methylpentane glass at 77 K, a mixture of the sample and very dilute 9,10-diphenylanthracene solution (optical density ~0.1 at 375 nm) was used, i.e., the diphenylanthracene was used as an internal fluorescence standard ($\Phi_F = 1.0$). The absorption spectrum of the mixture can be fitted very well as a sum of the spectra of 9,10-diphenylanthracene and the sample. For dilute samples of $Si_{16}Me_{34}$, the integrated fluorescence spectral ratio between sample and standard remained essentially constant as the solution containing a mixture of the sample and the diphenylanthracene was gradually diluted up to the detection limit of the fluorescence spectrometer.

In the determination of fluorescence quantum yield as a function of excitation energy, fluorescence spectra of the sample without the diphenylanthracene were measured at a series of excitation energies ($\tilde{\nu}^{EXC}$) in the ratioing mode of the fluorescence spectrometer that corrects exciting light intensities automatically. The nonlinear instrumental response for emission intensities at different wavelengths was corrected by predetermined correction factors. The relative fluorescence quantum yields were then calculated from the ratio of the corrected spectral area and the absorbance at the corresponding excitation energy and adjusted to the absolute fluorescence quantum yields on the basis of the separately determined $\Phi_F$ value at the absorption maximum.

Fluorescence lifetimes were measured by using the time-correlated single photon counting spectrometer at the Center for Fast Kinetics Research at the University of Texas at Austin. The excitation source was a cavity-dumped Rhodamine-B dye laser synchronously pumped by a Coherent Antares Nd:YAG laser mode-locked at ca. 86 MHz. Fluorescence decays were monitored by a Hamamatsu R1564U microchannel plate photomultiplier tube at right angles to the excitation source. Monochromator and cutoff filters were used for the selection of the emission energy and the emission energy region.

Polarized fluorescence spectra of $Si_{16}Me_{34}$ at 77 K were measured on a home-built fluorescence spectrometer which has been described elsewhere.[11] The experiment was carried out with an angle $\theta$ of 25° between the exciting and the observed beams and evaluated using the equation[17]

$$(I_\parallel^{iso}/I_\perp^{iso})^2 \cos^2\theta + (I_\parallel^{iso}/I_\perp^{iso}) \sin^2\theta - (I_{VV}I_{HH})/(I_{VH}I_{HV}) = 0 \quad (1)$$

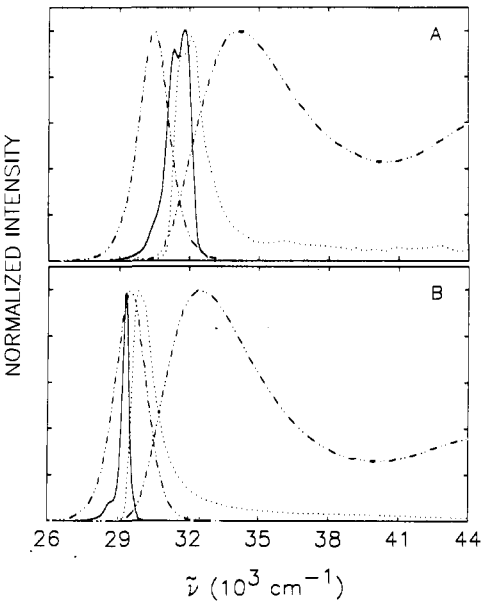


**Figure 1.** Absorption and fluorescence spectra of (A) $Si_{16}Me_{34}$ ($1.6 \times 10^{-7}$ M) and (B) $[SiMePr]_x$ ($1.5 \times 10^{-6}$ M SiMePr) in room-temperature hexane solution (----) and in 77 K 3-methylpentane glass (absorption, ···; fluorescence, —). Excited at absorption maxima.

**Table I.** Absorption and Fluorescence of $Si_{16}Me_{34}$ and $[SiMePr]_x$

| | ABS | | | FLSC | |
|---|---|---|---|---|---|
| | $\tilde{\nu}_{max}^{ABS}$ (cm$^{-1}$) | $\Delta\tilde{\nu}^a$ (cm$^{-1}$) | $\epsilon_{max}{}^b$ | $\tilde{\nu}_{max}^{EM}{}^c$ (cm$^{-1}$) | $\Delta\tilde{\nu}^a$ (cm$^{-1}$) |
| In Room-Temperature Solution | | | | | |
| $Si_{16}Me_{34}$ | 34 100 | 6200[d] | 4250 | 30 500 | 1500 |
| $Si_{16}Me_{34}$[e] | 33 900 | 1000 | | 28 900 | 1300 |
| $[SiMePr]_x$ | 32 500 | 5000[d] | 6600 | 29 500 | 1500 |
| In 77 K 3-Methylpentane Glass | | | | | |
| $Si_{16}Me_{34}$[f] | 32 100 | 1400 | | 31 750 | 1100 |
| | 31 700(sh) | | | 31 300 | |
| $Si_{16}Me_{34}$[g] | 32 100 | 1400 | | 31 200 | 1200 |
| | 31 700(sh) | | | 31 700(sh) | |
| $Si_{16}Me_{34}$[h] | 34 600 | 900 | | 30 000 | 400 |
| | | | | 29 400(Si–C?) | |
| $Si_{16}Me_{34}$[e] | 34 600 | 1200 | | 30 000 | 700 |
| $[SiMePr]_x$ | 29 900 | 1100 | | 29 300 | 350 |

[a] Full width at half-maximum. [b] Per Si unit. [c] Excited at the corresponding absorption maximum. [d] 3900 and 3500 cm$^{-1}$ for $Si_{16}Me_{34}$ and $[SiMePr]_x$, respectively, if the Gaussian first absorption band is assumed. [e] Solid. [f] Dilute solution. [g] Concentrated solution, rapid cooling. [h] Concentrated solution, slow cooling.

where $I_{IJ}$ (I, J = V, H) is the observed fluorescence intensity and the subscripts indicate the polarization directions of the excitation (first) and emission (second) polarizers (V = vertical, H = horizontal). $I_\parallel^{iso}$ and $I_\perp^{iso}$ obtained from eq 1 were used to calculate the degree of fluorescence polarization: $P = (I_\parallel^{iso} - I_\perp^{iso})/(I_\parallel^{iso} + I_\perp^{iso})$.

## Results

**Room-Temperature Spectra in Dilute Hexane Solutions. (A) Absorption and Fluorescence.** As shown in Figure 1 and Table I, $Si_{16}Me_{34}$ has a strong broad and structureless absorption peak comparable to that of the high molecular weight polymer $[SiMePr]_x$, but blue-shifted. Also shown in Figure 1 and Table I is the fluorescence of $Si_{16}Me_{34}$ and $[SiMePr]_x$ excited at their corresponding absorption maxima $\tilde{\nu}_{max}^{ABS}$. The emission of $Si_{16}Me_{34}$ is broad, Gaussian-like, and very similar to that of $[SiMePr]_x$ and those of the poly(di-*n*-alkylsilane)s reported previously.[4-6a,11] The emission band widths are significantly narrower than the corresponding first absorption band widths. Like the fluorescence spectra and fluorescence excitation spectra of high molecular

(16) Parker, C. A. *Photoluminescence of Solutions*; Elsevier: Amsterdam, 1968.

(17) Michl, J.; Thulstrup, E. W. *Spectroscopy with Polarized Light*; VCH Publishers, Inc.: New York, 1986.

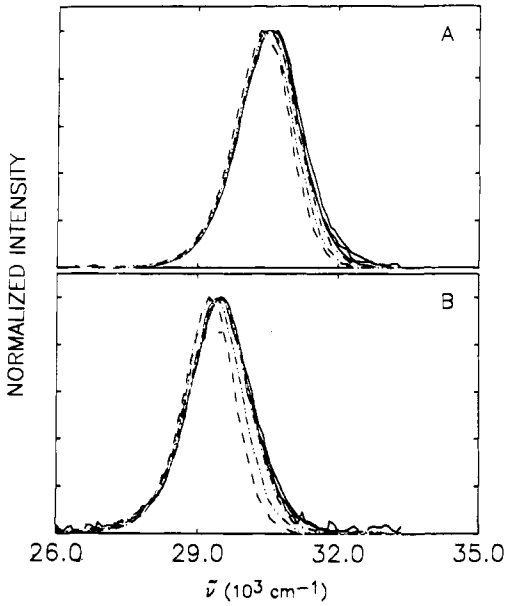


**Figure 2.** Excitation energy dependence of the fluorescence spectra of (A) $Si_{16}Me_{34}$ (from left to right, $\tilde{\nu}^{EXC}$ = 30 800, 31 200, 31 700, 32 200, 33 900, and 39 200 cm$^{-1}$) and (B) $[SiMePr]_x$ (from left to right, $\tilde{\nu}^{EXC}$ = 29 400, 30 300, 31 200, 32 200, 35 100, and 40 000 cm$^{-1}$) in hexane solution at room temperature.

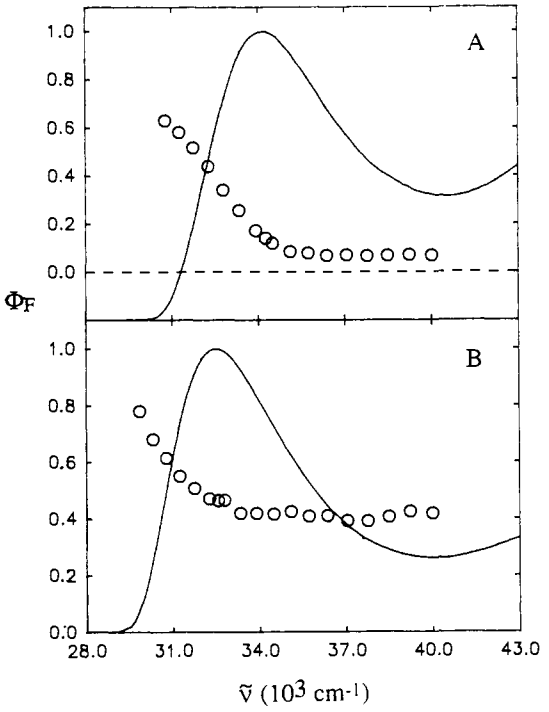


**Figure 3.** Excitation energy dependence of fluorescence quantum yields of (A) $Si_{16}Me_{34}$ and (B) $[SiMePr]_x$ in hexane solution at room temperature.

weight polymers, those of $Si_{16}Me_{34}$ are independent of sample concentration in the range examined ($(2 \times 10^{-7})$–$(5 \times 10^{-6})$ M).

Normalized fluorescence spectra of $Si_{16}Me_{34}$ and $[SiMePr]_x$ at representative choices of $\tilde{\nu}^{EXC}$ are compared in Figure 2. The spectral shape of $Si_{16}Me_{34}$ emission depends on the excitation energy in the same characteristic fashion as that of $[SiMePr]_x$ and other high molecular weight poly(di-*n*-alkylsilane)s.[11] As Figure 2 shows, all of the spectra measured at $\tilde{\nu}^{EXC} > \tilde{\nu}^{ABS}_{max}$ are essentially identical, and the spectra measured at $\tilde{\nu}^{EXC} < \tilde{\nu}^{ABS}_{max}$ change continuously with $\tilde{\nu}^{EXC}$, with the blue edge receding as $\tilde{\nu}^{EXC}$ decreases and the red onset hardly changing at all.

**(B) Fluorescence Quantum Yield and Lifetime.** The fluorescence quantum yields of both $Si_{16}Me_{34}$ and $[SiMePr]_x$ depend strongly on $\tilde{\nu}^{EXC}$. The plots of $\Phi_F$ against $\tilde{\nu}^{EXC}$ (Figure 3) are similar to those obtained for poly(di-*n*-alkylsilane)s.[6a,11] In each plot, there is a plateau region for $\tilde{\nu}^{EXC} > \tilde{\nu}^{ABS}_{max}$, where $\Phi_F$ is relatively small: about 0.07 and 0.4 for $Si_{16}Me_{34}$ and $[SiMePr]_x$, respectively. Typical values for poly(di-*n*-alkylsilane)s[11] are 0.25–0.4. At approximately $\tilde{\nu}^{EXC} = \tilde{\nu}^{ABS}_{max}$, the fluorescence quantum yields start to increase continuously with decreasing $\tilde{\nu}^{EXC}$. At the red edge of the absorption spectrum, the limiting $\Phi_F$ value for $Si_{16}Me_{34}$, $\Phi_F$ = 0.63 ($\tilde{\nu}^{EXC}$ = 30 800 cm$^{-1}$), is close to that for $[SiMePr]_x$, $\Phi_F$ = 0.8 ($\tilde{\nu}^{EXC}$ = 29 850 cm$^{-1}$). Typical values for poly(di-*n*-alkylsilane)s are 0.6–0.7.[11]

The fluorescence decay of $Si_{16}Me_{34}$ is essentially independent of the excitation energy and the monitored emission frequency. It fits a single exponential function with a lifetime of $\tau_F$ = 179 ± 20 ps (Table II). The value for $[SiMePr]_x$ is 226 ± 20 ps.

**Low-Temperature (77 K) Spectra in 3-Methylpentane Glass.** The absorption and emission properties of $Si_{16}Me_{34}$ in low-temperature 3-methylpentane solution and glass are different from those in room-temperature solution in that they depend strongly on the concentration of the sample and, for concentrations above $2 \times 10^{-7}$ M, also on its thermal history. In order to obtain results pertaining to isolated solute molecules, the samples must be very dilute.

The shape of the low-temperature absorption spectrum of a rapidly cooled sample is independent of concentration at concentrations lower than about $5 \times 10^{-6}$ M. We were able to record it reliably down to $1.6 \times 10^{-7}$ M. The height of its 32 100 cm$^{-1}$ peak obeys Beer's law (Figure 4). Deviations from Beer's law

**Table II.** Fluorescence Lifetimes of $Si_{16}Me_{34}$ and $[SiMePr]_x$[a]

| | | $\tilde{\nu}^{EXC}$ (cm$^{-1}$) | $\tilde{\nu}^{EM}$ (cm$^{-1}$) | $\tau_F$ (ps)[b] |
|---|---|---|---|---|
| $Si_{16}Me_{34}$ | RT | 35 100 | <27 800 | 166 |
| | | 34 500 | <31 300 | 179 |
| | | 33 300 | <27 800 | 170 |
| | 77 K[c] | 34 500 | 32 300 | 279 |
| | | | 31 700 | 250 |
| | | | 30 800 | 224 |
| | | 33 300 | 31 700 | 210 |
| | | | 30 300 | 236 |
| | | 31 700 | 30 800 | 200 |
| | 77 K[d] | 32 800 | 30 300 | 240 |
| | | 34 500 | 31 300 | 260 |
| | 77 K[e] | 34 500 | 30 100 | 650[f] |
| $[SiMePr]_x$ | RT | 34 500 | <31 300 | 226 |

[a] Room-temperature (RT) values are in hexane and 77 K values are in 3-methylpentane glass. [b] ±20 ps. [c] Dilute solution. [d] Concentrated solution, rapid cooling. [e] Concentrated solution, slow cooling. [f] Grow-in time constant of 160 ps.

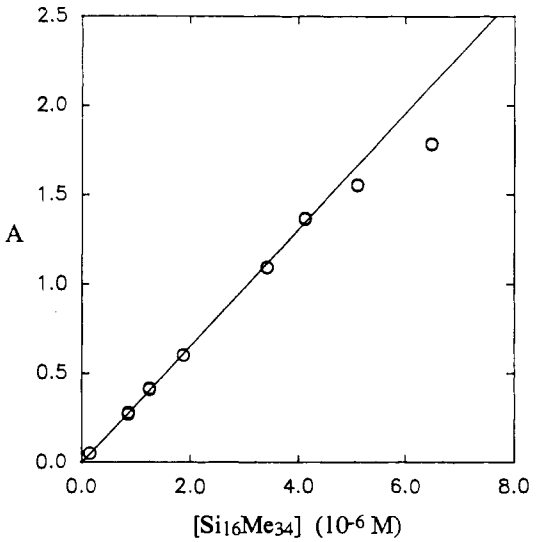


**Figure 4.** Absorbance at the ~32 100 cm$^{-1}$ maximum of $Si_{16}Me_{34}$ in 77 K 3-methylpentane glass as a function of sample concentration of a rapidly cooled sample.

occur only at higher concentrations, with the 32 100 $cm^{-1}$ peak absorbance lower than expected. Although some of the deviation may be due to instrumental error, it is probably significant that at the same time, a new sharp absorption peak appears at 34 600 $cm^{-1}$.

Comparison with the spectra of a solid film, discussed below, showed that the material responsible for the absorbance changes that occur above $\sim 5 \times 10^{-6}$ M consists of microscopic solid particles of $Si_{16}Me_{34}$, which precipitate from the solution upon cooling in a form invisible to the naked eye. The exact concentration at which a deviation from linear Beer's law behavior sets in, and the 34 600 $cm^{-1}$ peak of the solid appears, depends on the rate of cooling. This is somewhat slower in a square 1-cm cell, used to obtain the data of Figure 4, and faster in a flat 2-mm cell. In the latter, a $4.7 \times 10^{-6}$ M solution is still free of the complications caused by precipitation of microcrystals, and we refer to it below as a typical "concentrated solution". We refer to the $1.6 \times 10^{-7}$ M solution as a typical "dilute solution". In the case of the latter, the absorption spectra do not depend on the rate of cooling.

While the absorption spectra thus suggest the existence of only two regimes, true solution and colloidal solution with a precipitate, and show no distinction between the "concentrated" $4.7 \times 10^{-6}$ M solution and the "dilute" $1.6 \times 10^{-7}$ M solution, emission spectra clearly distinguish between the two, showing that the "concentrated" solution contains aggregates. Next, we shall describe the properties of the dilute solution, the concentrated solution, and the solid in a flat 2-mm cell.

**(A) Dilute Solution ($\leq 1.6 \times 10^{-7}$ M).** We have no reason to believe that the carrier of the absorption spectrum of a $1.6 \times 10^{-7}$ M solution is anything but the $Si_{16}Me_{34}$ monomer, most likely present as a mixture of conformers. The spectral peak is red-shifted from its room-temperature position (Figure 1). The absorption and fluorescence spectra of $[SiMePr]_x$ in 3-methylpentane glass at 77 K are also shown in Figure 1 for comparison.

Unlike the room-temperature absorption band of $Si_{16}Me_{34}$, its low-temperature spectral band is doubled. It peaks at 32 100 $cm^{-1}$ and has a distinct shoulder at about 31 700 $cm^{-1}$. In spite of its composite nature, the absorption band is quite narrow (FWHM = 1400 $cm^{-1}$). The fluorescence spectral shape is also independent of the manner of cooling, and the emission is again red-shifted relative to room temperature.

The fluorescence and fluorescence excitation spectra of the dilute sample depend strongly on the excitation and monitored emission energies, respectively, even in the region $\tilde{\nu}^{EXC} > \tilde{\nu}^{ABS}_{max}$. The overall width of the fluorescence spectrum decreases significantly as $\tilde{\nu}^{EXC}$ decreases, with the blue edge of the spectrum receding and the red edge of the spectrum hardly changing at all. A spectrum excited at the 32 100 $cm^{-1}$ absorption maximum is shown in Figure 1. It contains two peaks: one at 31 250 $cm^{-1}$ and one at 31 750 $cm^{-1}$. However, as shown in Figure 5, which displays the fluorescence spectra of the sample at several excitation energies, only the 31 250 $cm^{-1}$ fluorescence peak appears at low-energy excitation into the 31 700 $cm^{-1}$ absorption shoulder, and neither peak appears at high-energy excitation, which produces other, blue-shifted fluorescence bands with poorly defined structure, presumably due to contributions from a large number of distinct conformers.

This is further illustrated in Figure 6, which shows the fluorescence excitation spectra monitored at three different emission energies. The width and shape of the fluorescence excitation spectrum do not change very much with emission energy monitored, $\tilde{\nu}^{EM}$, and the spectrum is blue-shifted continuously as $\tilde{\nu}^{EM}$ increases. None of the fluorescence excitation spectra coincide with the absorption spectrum. In particular, they do not exhibit the 32 100 $cm^{-1}$ maximum characteristic of the latter, and their width is always narrower than that of the latter. It seems that the species responsible for the 32 100 $cm^{-1}$ absorption peak is nonfluorescent, or nearly so.

It appears that the combination of absorption, fluorescence, and fluorescence excitation spectra permits the identification of three distinct conformers with low-energy states and that a large number of others is also present, with somewhat higher excitation energies. The three that appear to be discernible are the following: (i) A, a species responsible for the 31 700 $cm^{-1}$ absorption shoulder and the 31 300 $cm^{-1}$ emission peak. Its absorption is probably

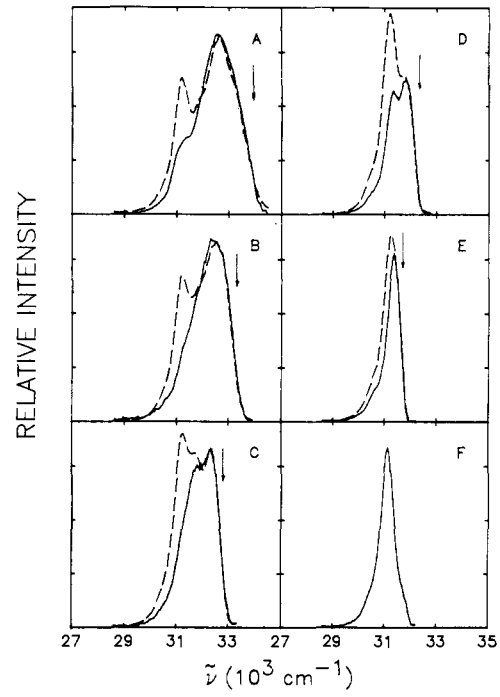


**Figure 5.** Fluorescence spectra of $Si_{16}Me_{34}$ in 77 K 3-methylpentane glass in dilute ($1.6 \times 10^{-7}$ M, —) and concentrated ($4.7 \times 10^{-6}$ M, ---) solutions at $\tilde{\nu}^{EXC}$ of (A) 33 900, (B) 33 300, (C) 32 800, (D) 32 300, and (E) 31 700 $cm^{-1}$, as marked by arrows. The spectrum in part F is the average of the difference between the spectra of the concentrated and the dilute samples shown in parts A–E.

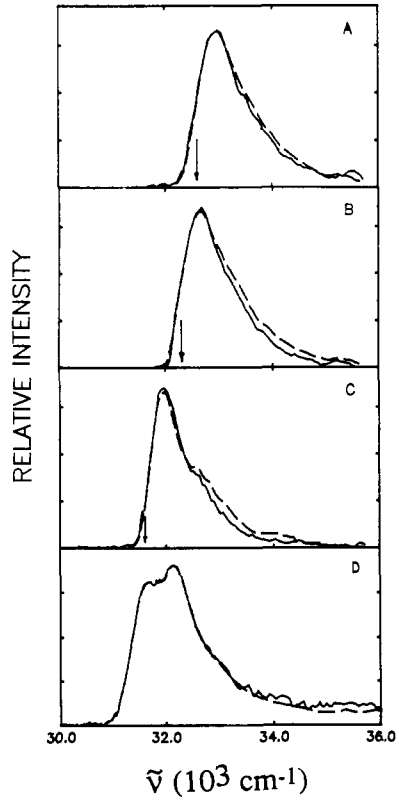


**Figure 6.** Fluorescence excitation spectra of $Si_{16}Me_{34}$ in 3-methylpentane glass at 77 K in dilute ($1.6 \times 10^{-7}$ M, —) and concentrated ($4.7 \times 10^{-6}$ M, ---) solutions at $\tilde{\nu}^{EM}$ of (A) 32 600, (B) 32 300, and (C) 31 600 $cm^{-1}$ as marked by arrows. (D) Absorption spectra.

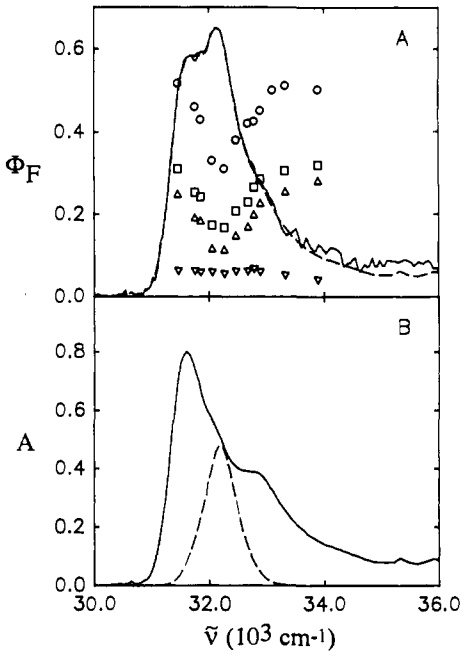


**Figure 7.** (A) Fluorescence quantum yield of $Si_{16}Me_{34}$ in 3-methylpentane glass at 77 K as a function of $\tilde{\nu}^{EXC}$: the observed $\Phi_F$ values for the dilute (○) and the concentrated (□) solutions under rapid cooling conditions. Decomposition of the latter into two components, the monomer (△) and the dimer (▽), is shown. The absorption spectra of the dilute (—) and the concentrated (---) samples are also shown. (B) Decomposition of the absorption spectrum into those of the fluorescent (—, A, B) and nonfluorescent (---, C) conformers.

well approximated by the excitation curve in Figure 6C and its fluorescence by the curve in Figure 5E. (ii) B, a species responsible for the fluorescence peak at 31 750 cm$^{-1}$. Its fluorescence can be approximated by subtracting the spectral curve in Figure 5E from that of Figure 5D. Its absorption appears to peak somewhere between 32 500 and 33 000 cm$^{-1}$. (iii) C, a nonfluorescent species responsible for the absorption peak at 32 100 cm$^{-1}$.

The fluorescence quantum yield of the dilute sample was determined as a function of $\tilde{\nu}^{EXC}$ (Figure 7A). Except for a dip near the 32 100 cm$^{-1}$ absorption maximum, the yield is almost constant at ~0.5. It seems reasonable to attribute the dip to absorption by the nonemissive species C. For an optically thin sample,

$$A^C(\tilde{\nu}) = A^{obsd}(\tilde{\nu})[1 - \Phi_F^{obsd}(\tilde{\nu})/\Phi_F(\tilde{\nu})] \qquad (2)$$

where $A^{obsd}(\tilde{\nu})$ and $A^C(\tilde{\nu})$ are the observed absorbance and the absorbance of the nonemissive species C, respectively, and $\Phi_F^{obsd}(\tilde{\nu})$ and $\Phi_F(\tilde{\nu})$ are the measured fluorescence quantum yield and the yield that would be observed in the absence of C, respectively. Assuming that the quantum yield would be constant at 0.5 if it were not for the presence of C, i.e., $\Phi_F(\tilde{\nu}) = 0.5$, the absorption spectra of C and of the sum of all the emissive species can be derived and are shown in Figure 7B. Although only three of a large number of species undoubtedly present have been tentatively identified, they account for the bulk of the absorption intensity.

The polarization degree of the fluorescence is close to $^1/_3$, but we were not able to measure it accurately.

The fluorescence decay of the dilute solution was measured at several excitation energies and different monitored emission energies. The decay curves can be deconvoluted from the instrumental response with a single exponential function if the experimental conditions for measurement of the decay and measurement of the instrumental response are duplicated very carefully, although they undoubtedly are due to simultaneous emission from two or more species, except perhaps for the measurement on species A (200 ps). As shown in Table II, the fluorescence lifetime is only very weakly dependent on the excitation and emission energies, with an average $\tau_F$ value of 230 ± 30 ps, but it appears to decrease distinctly as the excitation energy decreases, so that A rather than B and C is excited. It appears that the lifetime of B is somewhat longer than that of A. The spectral characteristics of the conformers A–C are summarized in Table III.

**(B) Concentrated Solution ($4.7 \times 10^{-6}$ M), Rapid Cooling.** Figure 7A shows that the absorption spectrum of the concentrated sample is essentially identical to that of the dilute one. Similarly, for all monitored emission energies, the fluorescence excitation spectra are essentially identical to the spectra of the monomer in the dilute ($1.6 \times 10^{-7}$ M) sample (Figure 6).

However, at any excitation energy, the fluorescence spectrum is different from that of the dilute sample (Figure 5). While these fluorescence spectra depend on the excitation energy in a fashion similar to the spectra of the dilute sample, they differ by the presence of a 31 200 cm$^{-1}$ peak at all excitation energies (Figure 5). Subtraction of the fluorescence spectrum of the monomer from that of the rapidly cooled concentrated solution recorded at the same excitation energy results in a residual spectrum which is nearly independent of the excitation energy. The average of these residual spectra, shown in Figure 5F, is a Gaussian-like peak centered at about 31 200 cm$^{-1}$ (321 nm) with FWHM of 650 cm$^{-1}$. It is perhaps accidental that this peak is very similar to the emission spectrum of the monomeric species A. For brevity, we shall refer to the high-concentration species responsible for the emission shown in Figure 5F as the "dimer", although it may consist of more than two $Si_{16}Me_{34}$ molecules.

The total fluorescence quantum yield of the sample is lower than that of the dilute sample at the same excitation energy, and its dependence on excitation energy is essentially parallel to that of the dilute sample (Figure 7A). Since each fluorescence spectrum can be decomposed into two spectra, one corresponding to the dilute sample (monomer spectrum) and one corresponding to the fluorescence band shown in Figure 5F (dimer spectrum), the total $\Phi_F$ can also be decomposed into the fluorescence quantum yields of the two spectral carriers according to their fractional contributions to the overall fluorescence spectrum. The $\Phi_F$ values of each component are shown in Figure 7A. The quantum yield of the dimer is about 0.06. It is independent of the excitation energy, making the excitation energy dependence of the $\Phi_F$ values for the monomer contribution parallel to that of the total $\Phi_F$.

Fluorescence decays of the rapidly cooled concentrated sample were measured at two excitation energies and different monitored emission energies. The decay traces were fitted by a single exponential function, yielding very similar $\tau_F$ values (Table II).

Fluorescence polarization was measured at $\tilde{\nu}^{EXC} = 33\,300$ cm$^{-1}$. The observed polarized fluorescence spectra are superpositions of the monomer emission ($I_{IJ}^m$) and the dimer emission ($I_{IJ}^d$).

$$I_{IJ}(\tilde{\nu}) = I_{IJ}^m(\tilde{\nu}) + I_{IJ}^d(\tilde{\nu}) \qquad (I,J = V,H) \qquad (3)$$

Even if the polarization of each emitting species is independent of the emission energy monitored, the observed degree of polarization $P$ will depend on it. Indeed, there are two regions in the plot of $P$ against $\tilde{\nu}^{EM}$ (Figure 8A). In the region dominated by the monomer fluorescence, the $P$ values are quite high, about 0.35. This compares well with the approximate value of $^1/_3$ estimated from the measurement on a dilute sample, which did not depend on $\tilde{\nu}^{EM}$. In the $\tilde{\nu}^{EM} < 31\,300$ cm$^{-1}$ region, in which the dimer fluorescence band dominates, the $P$ values are only about 0.1. Assuming that the $P$ value of the monomer remains constant at 0.35 even in this region, as suggested by the measurement on a dilute sample, a spectral decomposition can be achieved by subtracting the polarized spectrum of the monomer from each of the polarized fluorescence spectra. The degree of polarization values for the monomer and the dimer were then calculated according to eq 1 (Figure 8B). Within experimental uncertainties, the $P$ value of the dimer fluorescence is also independent of $\tilde{\nu}^{EM}$. This emission is essentially totally depolarized ($P \simeq 0$).

The concentration dependence of the monomer and dimer fluorescence quantum yields of $Si_{16}Me_{34}$ at three excitation energies is shown in Figure 9. In the high-dilution limit, only the monomer emission is observed. In the high-concentration limit—but before precipitation sets in—the dimer emission yield is about 0.06.

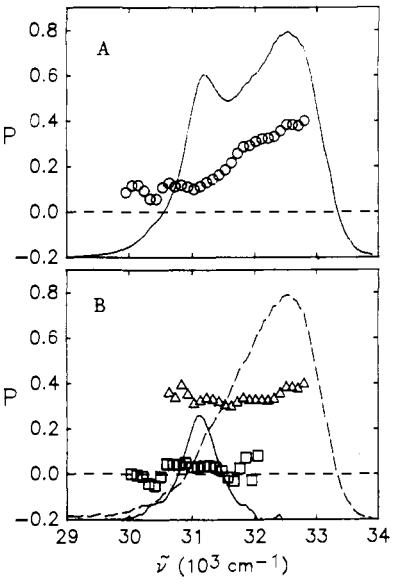


**Figure 8.** Degree of fluorescence polarization $P$ of $Si_{16}Me_{34}$ in 3-methylpentane at 77 K as a function of $\tilde{\nu}^{EM}$ ($\tilde{\nu}^{EXC}$ = 33 300 cm$^{-1}$): (A) fluorescence spectrum and observed $P$ values; (B) deconvoluted spectra and $P$ values for the monomer (---, △) and for the dimer (—, □).

**Table III.** Spectral Characteristics of $Si_{16}Me_{34}$ Conformers and Aggregates

| | $\tilde{\nu}^{ABS}_{max}$ (cm$^{-1}$) | $\tilde{\nu}^{EM}_{max}$ (cm$^{-1}$) | $\Phi_F$ | $\tau_F$ (ps) |
|---|---|---|---|---|
| A | 31 700 | 31 300 | ~0.5 | 230[a] |
| B | 32 800 | 31 750 | ~0.5 | 230[a] |
| C | 32 100 | nonemissive | | |
| dimer | ?[b] | 31 200 | ~0.06 | ~260 |
| microcrystal | 34 600 | 30 000 | 0.26 | 650[c] |

[a] Average values. [b] The dimer could be disorganized clusters of $Si_{16}Me_{34}$ molecules in loose contact, which leaves their absorption spectra unperturbed. It is also possible that the absorption peak of the dimer is nearly identical to that of A (see text). [c] Grow-in time constant of 160 ps.

The spectral characteristics of the dimer are also given in Table III for comparison. Although the monomeric species A and the dimer emit at similar energies and with similar lifetimes, they are spectroscopically distinct. They have rather different fluorescence quantum yields, polarization, and excitation spectra. Most importantly, if the fairly intense dimer emission observed at the higher concentrations were simply due to increased amounts of A relative to other conformers, the absorption band associated with A would have to appear with the corresponding increased intensity as well. Yet, the absorption as well as excitation spectra are independent of concentration in the relevant range.

It is quite possible and perhaps even likely that A represents a key structural element in the architecture of the emitting dimer, imparting to it some of its own spectral characteristics, but a single molecule of A cannot be the dimer's only constituent.

**(C) Concentrated Solution, Slow Cooling.** When a 4.7 × 10$^{-6}$ M solution was cooled to 77 K slowly, the absorption spectra recorded during the cooling process showed gradual narrowing and slight blue-shifting of the room-temperature first absorption band and a significant decrease of absorption in the higher energy region. In about half an hour (at −120 to −140 °C), the absorption spectrum became a sharp Gaussian-like band with a maximum at 34 600 cm$^{-1}$ (FWHM ~900 cm$^{-1}$) and a weak tail reaching to about 30 000 cm$^{-1}$. Subsequent cooling to 77 K hardly changed the absorption spectrum at all (Figure 10A). With excitation at the absorption maximum, the fluorescence spectra before and after the cooling to 77 K were also nearly identical. As shown in Figure 10A, the fluorescence spectrum consists of a sharp band (FWHM = 400 cm$^{-1}$) at 30 000 cm$^{-1}$, which is 4600 cm$^{-1}$ red-shifted from the absorption maximum, and a much weaker peak at ~29 400 cm$^{-1}$. It is independent of excitation energy, as is the

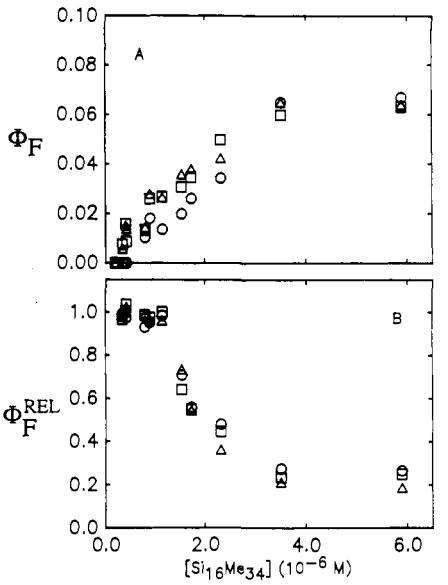


**Figure 9.** Fluorescence quantum yields of $Si_{16}Me_{34}$ in 77 K 3-methylpentane glass as a function of sample concentration at $\tilde{\nu}^{EXC}$ = 33 300 (○), 32 800 (△), and 32 300 cm$^{-1}$ (□) for (A) the dimer and (B) the monomer (relative $\Phi_F$ only).

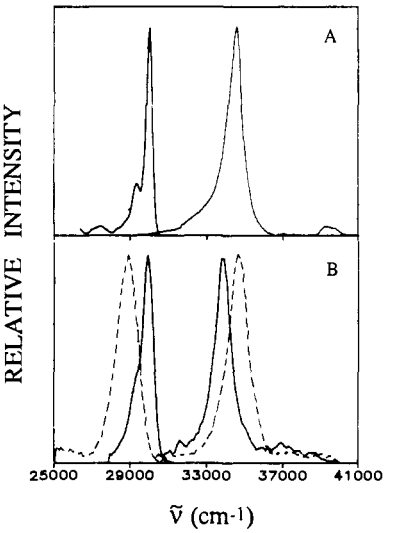


**Figure 10.** Absorption and fluorescence spectra of $Si_{16}Me_{34}$: (A) slowly cooled, concentrated (4.7 × 10$^{-6}$ M) sample; (B) solid film on quartz surface at room temperature (---) and 77 K (—).

fluorescence quantum yield, $\Phi_F$ = 0.26 ± 0.05.

The fluorescence decay of the slowly cooled sample is also independent of excitation energy. The decay curves monitored at the first (30 000 cm$^{-1}$) and the second (29 400 cm$^{-1}$) emission bands, excited at 34 600 cm$^{-1}$, were essentially identical. Each of them could be fitted approximately with a double exponential function, corresponding to a grow-in time constant of about 160 ps and a decay lifetime of about 650 ps (Figure 11).

The degree of polarization of the fluorescence of the slowly cooled sample is 0.33, independent of the excitation energy and of the emission energy monitored.

If the sample concentration is increased above 4.7 × 10$^{-6}$ M, corresponding to the curved region in Figure 4, the absorption and emission properties observed with slow cooling remain basically the same. At these higher concentrations, some of these properties, particularly the occurrence of the 34 600 cm$^{-1}$ absorption band, persist even under rapid cooling conditions.

For concentrations between 4.7 × 10$^{-6}$ and 1.6 × 10$^{-7}$ M, intermediate results were obser ed. Slow cooling of these samples did not exclusively generate the characteristic absorption band at 34 600 cm$^{-1}$ and fluorescence bands at 30 000 and 29 400 cm$^{-1}$,

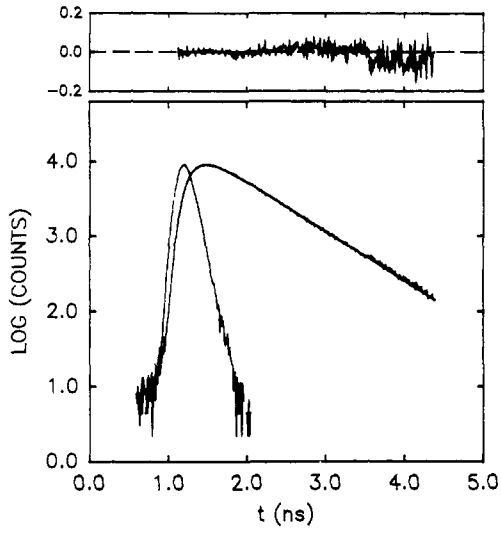


**Figure 11.** Fluorescence decay of $Si_{16}Me_{34}$ in 77 K 3-methylpentane glass, slowly cooled, concentrated ($4.7 \times 10^{-6}$ M) sample ($\tilde{\nu}^{EXC}$ = 34 500 $cm^{-1}$, $\tilde{\nu}^{EM}$ = 30 100 $cm^{-1}$). The instrumental response function and decay curve are on log scale. The fitted decay curve has a grow-in time constant of 160 ps and a decay lifetime of 650 ps. The top insert is the residual.

and it took a longer time for these spectral bands to grow. There is also a correlation between intensities of the 31 200 $cm^{-1}$ fluorescence band and the 30 000 and 29 400 $cm^{-1}$ bands, depending on the cooling time. As the cooling rate decreases, the intensities of the 30 000 and 29 400 $cm^{-1}$ fluorescence bands increase and the intensity of 31 200 $cm^{-1}$ band decreases, showing that the generation of the former requires consumption of the latter. These were the results that initially suggested that precipitation occurs during the slow cooling process and that a solid is being observed. This was then confirmed by a direct comparison (Figure 10B).

At room temperature, a solid film of $Si_{16}Me_{34}$ has sharp Gaussian-like absorption and fluorescence peaks ($\tilde{\nu}^{ABS}_{max}$ = 33 900 $cm^{-1}$, FWHM = 1000 $cm^{-1}$, for absorption and $\tilde{\nu}^{EM}_{max}$ = 28 900 $cm^{-1}$, FWHM = 1300 $cm^{-1}$, for fluorescence). At 77 K, the solid film in liquid nitrogen has the absorption and fluorescence spectra shown in Figure 10B, nearly identical to those of the concentrated sample under the slow cooling conditions, except that the fluorescence spectrum of the solid film at 77 K is not as well resolved. Both absorption and fluorescence spectra of the solid film at 77 K are independent of the rate of cooling.

## Discussion

**Room Temperature. Poly(methylpropylsilane).** In order to set the stage for a discussion of the properties of $Si_{16}Me_{34}$, we first briefly summarize the photophysical behavior of high molecular weight poly(di-*n*-alkylsilane)s, as exemplified by $[SiMePr]_x$. In room-temperature solution, both the polymers with all alkyl groups equal[11] and others[4-6a] exhibit a fluorescence spectral shape, quantum yield, and degree of polarization that depend on the excitation energy in a very characteristic fashion.

Poly(methylpropylsilane) has been chosen in this study for comparison with $Si_{16}Me_{34}$ as it appears to be the closest tractable analogue of the extremely poorly soluble poly(dimethylsilane). Its photophysical properties are very similar to those of poly(di-*n*-alkylsilane)s with all alkyl groups equal.[11]

There are two distinct excitation energy regions: one below and the other above $\tilde{\nu}^{ABS}_{max}$. In the former region ($\tilde{\nu}^{EXC} > \tilde{\nu}^{ABS}_{max}$), the spectral shape and the quantum yield of the fluorescence are virtually independent of excitation energy (the "plateau region"), and the degree of fluorescence polarization is almost zero. In the latter region ($\tilde{\nu}^{EXC} < \tilde{\nu}^{ABS}_{max}$), the spectral shape of the fluorescence depends continuously on the choice of $\tilde{\nu}^{EXC}$, with the blue edge of the emission band receding as $\tilde{\nu}^{EXC}$ decreases, while the position of the red edge is affected much less. The fluorescence quantum yield $\Phi_F$ also changes with excitation energy in this region: it increases steeply and almost linearly as the excitation energy decreases, from a value of about 0.4 in the plateau region to about 0.8 in the edge limit. The degree of fluorescence polarization $P$ increases in this region as well and reaches values as high as 0.45 for excitation at the red onset of the absorption band. Combined with the observed emission lifetime of 226 ps, the red edge limit value yields a radiative lifetime of about 280 ps, which corresponds to an oscillator strength of about 2.4. The oscillator strength per silicon atom determined by integration of the first absorption band is $f$ = 0.155. Assuming that the contributions of the individual silicon units are strictly additive, the average lowest energy emitting chromophore in $[SiMePr]_x$ thus contains about 15.5 Si units. This can be compared with the value of about 20 Si units found in a similar fashion for poly(di-*n*-hexylsilane).[5]

The existence of the two regions for polysilanes has been accounted for by the modified segment model.[11] The bulk of the fluorescence must originate in the long segments regardless of the choice of excitation energy. For $\tilde{\nu}^{EXC} < \tilde{\nu}^{ABS}_{max}$, the strongly fluorescent long segment chromophores are selectively excited, resulting in a continuous shift of the blue edge of the emission band as $\tilde{\nu}^{EXC}$ decreases. For $\tilde{\nu}^{EXC} > \tilde{\nu}^{ABS}_{max}$, primarily weakly fluorescent short segment chromophores are excited, followed by a rapid energy transfer to a standard distribution of long segment chromophores in competition[9,18] with photochemical decay, intersystem crossing, and possibly internal conversion. The presence of rapid intrachain energy transfer is supported by the steady-state[4,5,10a,11] and time-resolved[10b,19] fluorescence depolarization measurements. The transfer of excitation energy to longer segments could occur by the exchange (Dexter) mechanism for nearby chromophores, by the dipole–dipole mechanism for more distant ones, and possibly also by changes in segment length resulting from bond torsions driven by the shape of the excited potential energy surface.

***n*-Permethylhexadecasilane.** The absorption and fluorescence behavior of $Si_{16}Me_{34}$ is similar to that of peralkylated polysilane high molecular weight polymers. The absorption maximum of $Si_{16}Me_{34}$ is only slightly blue-shifted from those of the high polymers. The maximum molar extinction coefficient per Si unit, 4250 for $Si_{16}Me_{34}$, is somewhat smaller than that of $[SiMePr]_x$ (6600 per Si unit) and those of poly(di-*n*-alkylsilane)s (close to 10 000 per Si unit). However, since the absorption peak of $Si_{16}Me_{34}$ is broader than those of the polymers, its integrated absorption intensity per Si unit ($f$ = 0.125) is only about 20% smaller than that of $[SiMePr]_x$ ($f$ = 0.155).

It is then natural to account for the absorption spectrum of $Si_{16}Me_{34}$ in room-temperature solution as due to an inhomogeneous mixture of conformers characterized by a distribution of nearly planar all-trans segment chromophores with different numbers of Si atoms. Apparently, the relative population of conformations containing long segments in $Si_{16}Me_{34}$ is smaller than in the polymers, resulting in a blue shift and increased width of the absorption band (Figure 1). There is evidence from fluorescence quenching experiments that the more compact conformers of $Si_{16}Me_{34}$ have a higher excitation energy than those that are more extended in space.[12]

The room-temperature fluorescence band of $Si_{16}Me_{34}$ has a much smaller width than the corresponding first absorption band (Figure 1A and Table I), suggesting a much narrower distribution of segment lengths in the emitting species. Such a difference has been observed in high molecular weight polymers also, but it is more pronounced here. In the polymers, it is attributable to intrachain energy transfer, which produces a fluorescent segment distribution weighted heavily toward the longest segments. In $Si_{16}Me_{34}$, for $\tilde{\nu}^{EXC} > \tilde{\nu}^{ABS}_{max}$, the emitting long segments can again be generated through intramolecular energy transfer from initially excited short segments. However, comparison with low-temperature spectra presented below suggests that they also are

(18) McKinley, A. J.; Karatsu, T.; Wallraff, G. M.; Miller, R. D.; Sooriyakumaran, R.; Michl, J. *Organometallics* **1988**, *7*, 2567. Karatsu, T.; Miller, R. D.; Sooriyakumaran, R.; Michl, J. *J. Am. Chem. Soc.* **1989**, *111*, 1140.

(19) Thorne, J. R. G.; Hochstrasser, R. M.; Zeigler, J. M. *J. Phys. Chem.* **1988**, *92*, 4275.

generated quite efficiently through adiabatic excited-state conformational changes that extend the length of a particular excited short segment at the expense of its neighbors, presumably producing primarily the all-trans conformer. The driving force for such conformational change is believed to be provided by the lower excitation energy of the longer segments. Combined with comparable ground-state energies, this results in an excited-state potential energy surface that favors the conformations with the longest straight segments.

In polymers, such conformational changes would be slower, because change at one gauche link usually requires changes at other links in the connected long chain. The larger Stokes shift in $Si_{16}Me_{34}$ (3600 $cm^{-1}$) compared with the Stokes shift in poly(di-*n*-alkylsilane)s (~2500 $cm^{-1}$) is consistent with the argument. For $\tilde{\nu}^{EXC} < \tilde{\nu}^{ABS}_{max}$, the long segments are directly excited according to their contributions to the absorption.

The dependence of fluorescence spectral shape on excitation energy (Figure 2) suggests that the number of silicon atoms in $Si_{16}Me_{34}$ is sufficient to let a longer segment chromophore and a shorter segment chromophore coexist in one molecule and is too large for all conformers to convert adiabatically to the most stable ones completely before emitting. This may be the primary reason for its fluorescence properties being so close to those of the polymers, in which energy transer to the very lowest energy chromophores is extensive but not quite complete before emission occurs. As in $[SiMePr]_x$ and poly(di-*n*-alkylsilane)s, for $\tilde{\nu}^{EXC} > \tilde{\nu}^{ABS}_{max}$, both the fluorescence spectrum and the quantum yield of $Si_{16}Me_{34}$ hardly change with excitation energy, corresponding to plateau regions in their excitation energy dependence (Figures 2 and 3). The existence of the plateau regions may be due to the same reason proposed for the polymers:[11] the excited short segments are believed to be effectively nonfluorescent, because their lowest excited singlet state is only weakly allowed.[11] The observed fluorescence originates from the excited longer segments which are populated extremely fast by intramolecular energy transfer from shorter ones and through adiabatic conformational change in the excited state.

To a degree, it is a matter of semantics whether the transformation of a higher excited state, in which excitation is largely localized in a shorter segment of a 16-silicon chain, to a lower excited state, in which excitation is largely localized in a longer segment of the same conformer, should be called internal conversion or energy transfer. We have chosen the latter in order to emphasize the relation to the high polymers.

The actual value of $\Phi_F$ in the plateau region is 6 times lower for $Si_{16}Me_{34}$ (0.07) than for the model polymer, $[SiMePr]_x$ (0.4). This suggests that adiabatic generation of long segment chromophores by conformational change is less efficient than energy transfer along the backbone of a polymer. Clearly, many of the conformer molecules that contain only short segments and are excited at $\tilde{\nu}^{EXC} > \tilde{\nu}^{ABS}_{max}$ undergo dark processes such as intersystem crossing, internal conversion, or photochemical reactions and do not straighten out to yield an excited conformer containing a long segment. Photochemical quantum yields have not yet been measured, but if anything, $Si_{16}Me_{34}$ is more photostable than the polymers.

For $\tilde{\nu}^{EXC} < \tilde{\nu}^{ABS}_{max}$, both the fluorescence spectral shape and the fluorescence quantum yield of $Si_{16}Me_{34}$ change continuously with excitation energy. As in the polymers, this can be attributed to a selective excitation of those conformers in the mixture that contain a long segment and incomplete adiabatic conversion to the most stable conformer before emission takes place. While the fluorescence quantum yield increases almost linearly with excitation energy to a value of 0.63 at $\tilde{\nu}^{EXC}$ = 30 800 $cm^{-1}$, the fluorescence lifetime remains essentially constant at 180 ps, close to the values observed for the polymers.[11]

Combined with the limiting fluorescence quantum yield of 0.63, the observed lifetime yields a radiative lifetime of 285 ps for the emitting long segment chromophore in $Si_{16}Me_{34}$. This is virtually identical to the value for $[SiMePr]_x$ and again translates into an oscillator strength of ~2.4, or 0.15 per Si unit. Clearly, there is little difference between the emitting chromophore in $Si_{16}Me_{34}$ and in $[SiMePr]_x$, not only in energy but also in intensity.

The oscillator strength calculated from the first absorption band of the $Si_{16}Me_{34}$ conformer mixture is ~2 (0.125 per silicon unit), somewhat smaller than that obtained from the radiative lifetime. This is reasonable as the long segment conformers, presumably formed before emission occurs, can be expected to have somewhat larger transition moments per silicon atom. The 20% discrepancy suggests a rough limit on the accuracy with which the 16–20 average length of a fluorescing segment in the polymers has been estimated using the assumption of a constant intensity increment per silicon atom.

As discussed for poly(di-*n*-alkylsilane)s,[11] the decoupling of the fluorescence lifetime and quantum yield is due to the fact that the former primarily reflects the properties of the long segments while the latter is affected also by the efficiency with which an originally excited short segment is transformed into an excited long segment.

**Low Temperature. Monomolecularly Dispersed $Si_{16}Me_{34}$.** In many respects, the photophysical behavior of a dilute $Si_{16}Me_{34}$ sample (the single-molecule form) in a 3-methylpentane glass at 77 K is similar to that of the high molecular weight polymers, but there are important differences too (Figure 1). Upon cooling, the absorption and fluorescence peaks of $Si_{16}Me_{34}$ become narrower. The former is shifted to the red, as is that of $[SiMePr]_x$ (Figure 1). Such thermochromic shifts are typical of the absorption peaks of many poly(dialkylsilane)s.[2,7,8] However, the fine structure in the low-temperature absorption, emission, and excitation spectra of $Si_{16}Me_{34}$, which permitted us to deduce the presence of the three major conformers A–C and numerous others, is without analogy in the spectra of the high polymers.

The oscillator strength deduced from the total absorption intensity is $f$ = 1.55. This can be separated in an approximate fashion into a contribution due to the main emissive species A and B on the one hand (1.21) and contribution due to the nonemissive species C on the other hand (0.34). Contributions from the higher energy conformers are of minor importance.

The oscillator strength associated with the main emissive species again compares fairly well with the value deduced from their emission properties. The fluorescence quantum yield of A and B is about 0.5. The fluorescence decay times of A and B do not appear to differ much, and we can take 230 ps as a reasonable average value. This leads to an estimated radiative lifetime of 460 ps, corresponding to an oscillator strength of 1.5.

In striking contrast to the absorption, the emission peak of $Si_{16}Me_{34}$ shifts strongly to the blue upon cooling, so that the Stokes shift is reduced dramatically. This is quite different from the behavior of $[SiMePr]_x$, whose emission peak shifts only very slightly to the red.

As in the polymers, the narrowing and thermochromic shift of the oligomer absorption are presumably due to going from a wide distribution of segment chromophores, many of which are short and absorb at higher energies, to a narrower distribution in which longer all-trans segments are more heavily represented. In some of the polymers with longer alkyl groups, a low-temperature form with a very narrow UV absorption band is observed in which only long segments are apparently present, but $Si_{16}Me_{34}$ does not show this type of behavior.

The striking temperature effect on the emission is interpreted most readily as due to an inhibition of adiabatic conformational transformations in the excited species by the high viscosity of the glassy medium. Now, the absorbing and the emitting conformations are one and the same, and the Stokes shift is small. Judging by their higher excitation energies, these conformations are nowhere nearly as extended as those that emit in room-temperature solution, and we do not believe that any one of the species A–C is the all-trans conformer, while the room-temperature emitting species could well be. The nature of the nonfluorescent species C is the most intriguing. Normally, we tend to attribute a lack of fluorescence to short chain chromophores, and yet C has a relatively low excitation energy.

The low absorbance at about 33 000 $cm^{-1}$ at low temperature, compared to room temperature, and the very different excitation

energy dependence of the fluorescence quantum yield in the two cases suggest that most of the conformers that contain short segments of all-trans bonds are less abundant at low temperature. The tremendous increase in the fluorescence quantum yield at 77 K relative to room temperature for $\bar{\nu}^{EXC}$ above the absorption maximum may be due to such greatly reduced abundance of poorly emissive conformers. Alternatively, it might be due to thermal activation barriers located in the way of nonradiative decay processes in the higher energy chromophores. There is evidence for such thermally activated internal conversion in the shorter oligosilanes, $Si_{10}Me_{22}$ and $Si_6Me_{14}$.[2a]

The fluorescence lifetime of $Si_{16}Me_{34}$ in low-temperature glass is only a little longer than in room-temperature solution, indicating the absence of thermally activated dark paths in the relatively low-energy chromophores. A similar observation has been reported for the high polymers.[19]

**Molecular Aggregates of $Si_{16}Me_{34}$.** The strong concentration dependence of $Si_{16}Me_{34}$ emission spectra in $\sim 10^{-6}$ M solutions, under conditions in which there is no evidence for solid particles and in the absence of analogous changes in the absorption spectra, is quite striking. It suggests the formation of a dimeric or more highly aggregated fluorophore, responsible for the 31 200 $cm^{-1}$ emission peak, when the sample is rapidly cooled to 77 K. Note, however, that the shape of the monomer part of the emission is independent of concentration at all excitation wavelengths (Figure 5). The results thus show that the relative proportions of the monomeric species A–C are concentration independent.

There are two obvious ways of accounting for the appearance of a dimer emission band in the absence of simultaneous changes in the shape of the absorption spectrum as a function of concentration in this region and for the linear dependence of the absorbance on the sample concentration, until at high concentrations precipitation of solid particles with very different spectra occurs (Figure 10).

(i) Since the emission peak of the dimer is nearly identical with that of the monomeric species A, its absorption peak could be too, both in wavelength and in absorbance per silicon atom. Then, the absorption peak would be due to the monomer at low concentrations, to the dimer at high concentrations, and to a mixture of the two at intermediate concentrations. The fluorescence quantum yield from the monomer, about 0.5, would undergo an apparent decrease with increasing concentration, while that from the dimer would undergo an apparent increase to the limiting value of about 0.06.

However, Figure 9 shows that the gradual conversion of the emission intensity from the monomeric to the dimeric type saturates at a concentration of about $3.5 \times 10^{-6}$ M, when the quantum yield of the monomer emission still has about 20% of its low-concentration limiting value. This can only be accommodated if one is willing to postulate that the dimer is responsible for two emissions, one of which is identical with that of the monomer. This appears unlikely, unless the dimer actually is an aggregate of many $Si_{16}Me_{34}$ units acting as an efficient antenna that harvests excitation energy for an emissive center responsible for the peak at 32 100 $cm^{-1}$. This then suggests a second way in which the observations can be accommodated.

(ii) The population of the true dimeric emissive center is very small, but the center is located inside a loose conglomerate of monomeric molecules which do not interact with each other sufficiently strongly for their absorption spectra to be modified significantly, but which do communicate by rapid energy transfer. The concentration of the dimeric emissive center is too low to be detected in the absorption spectrum, and it is immaterial whether or not it absorbs at the same energy as the monomer A. Due to energy transfer from the loosely associated monomers, the dimer could still be responsible for the observed relatively high emission quantum yield of 0.06. However, the harvesting is imperfect in that some of the monomer molecules fluoresce instead of transfer the excitation energy to the dimeric emissive center, accounting for the observed residual monomer fluorescence quantum yield of about 0.1 in the concentration region above $3.5 \times 10^{-6}$ M. This would not be surprising, considering the short low-temperature radiative lifetime of the monomer of about 450 ps. The fact that the fluorescence lifetime of the dimer is identical with that of the monomer within experimental error suggests that the radiative lifetime of the dimeric emissive center is even shorter and that the energy transfer to it is the rate-limiting step.

The observation that the dimer fluorescence is nearly completely depolarized agrees well with this picture if one assumes that there is no particular organization among the molecules participating in the energy-transfer process.

The absence of any dependence of the quantum yield of the dimer emission on excitation energy (Figure 7A) is striking. Either the nonemissive but absorbing species C is absent at higher concentrations or it is present but transfers energy to the dimeric emissive center just as efficiently as other monomeric species present. The first of these possibilities is not very appealing, as the absence of C at higher concentrations should be reflected in the absorption spectrum. It appears that the energy transfer from C to A, which has lower excitation energy, is extremely efficient within the loose cluster.

At this time, we are not able to provide a specific proposal for the structure of the dimeric center. From its excitation energy, it is unlikely that its constituents are in the fully extended zig-zag conformation. If its spectral properties are dominated by dipole–dipole coupling, its short radiative lifetime suggests that it is unlikely to consist of two or more $Si_{16}Me_{34}$ chains lying parallel side by side. It appears more likely that it could consist of two or more chains aligned end-to-end, perhaps with some overlap of the ends.

**Solid Particles of $Si_{16}Me_{34}$.** Slow cooling of concentrated $Si_{16}Me_{34}$ solution apparently allows the clusters to develop further into microcrystals which have essentially the same photophysical properties as a neat film of the solid. At high sample concentration ($>4.7 \times 10^{-6}$ M), the precipitation of solid particles occurs even when the sample is cooled rapidly, corresponding to the curved region in Figure 4. The absorption spectrum of the solid contains an intense peak at 34 600 $cm^{-1}$ with a weak long tail on the red edge, terminating near 30 000 $cm^{-1}$. This is the pattern expected from an excitonic interaction between extended parallel chains arranged side by side. The optically forbidden lowest energy excited state resulting from the interaction is revealed clearly in the fluorescence spectrum. The fine structure in the emission corresponds to a 600 $cm^{-1}$ vibration and thus lies in the region of Si–C stretching vibrations.

The grow-in portion of the fluorescence observed in the time-resolved experiment likely represents the energy migration process in the solid before an energy trap is reached. The energy trapping sites, presumably defects in the crystal structure, then fluoresce with a much longer lifetime. Although we cannot determine the radiative lifetime of the trap, it is clearly quite long. Perhaps the traps are formed by parallel chains located a little closer to each other than elsewhere in the solid. The high degree of polarization observed for the fluorescence suggests that the solid is highly ordered, such that the energy transfer occurs primarily among parallel chains. The solid particles precipitated from the solution are thus perhaps best called microcrystals. The structure of a crystal of $Si_{16}Me_{34}$ is not known, but the absorption and emission data would be nicely accommodated by stacks of parallel chains. A more detailed study of the solid would clearly be worthwhile.

Although the aggregation phenomena described here for $Si_{16}Me_{34}$ are somewhat reminiscent of those known for the high polymers,[8] the spectral properties of solid $Si_{16}Me_{34}$ are very different from those of the neat polymers. This suggests considerable structural differences.

## Conclusions

There is a striking similarity between the photophysical behavior of $Si_{16}Me_{34}$ and that of the high molecular weight polymer $[SiMePr]_x$, but some of it is superficial and due to different underlying physical processes. The difference is revealed clearly in low-temperature measurements in a high-viscosity medium.

We believe that the fundamental cause of the spectral similarity is the fact that in room-temperature solution both systems represent similar statistical collections of the same type of chromo-

phoric oligosilane segments, each of which is characterized by a single intense absorption and emission contribution of the $\sigma$-$\sigma^*$ type at an energy dictated by its length and exact geometry. The similarity of the two assemblies accounts for the similarity of the observed absorption spectra.

The fundamental difference between the two cases is the absence of covalent links between some of the individual chromophoric segments in the case of the hexadecasilane model. This makes little difference in absorption, but has two important consequences that are potentially important for emission spectra. However, their effects compensate: the absence of the links limits the extremely fast intersegment energy transfer known from the polymer to a range of no more than 16 silicon atoms, and it greatly enhances conformational mobility within such groups of 16 silicon atoms in media of low viscosity.

In both cases, emission from a room-temperature solution occurs primarily but not exclusively from about 16-silicon chromophoric segments of the lowest excitation energy (presumably all-trans), and the cutting of the polysilane backbone into 16-silicon pieces thus has almost no effect. In the polymer, excitation in any chromophoric segment is largely transferred to the lowest energy chromophores by energy transfer over considerable distances along the backbone with some emission occurring in competition, resulting in a weak excitation energy dependence of the fluorescence shape. In hexadecasilane, the excitation of any chromophoric segment is transformed into excitation of the lowest energy chromophores by an adiabatic distortion of the molecular geometry of the now freely mobile 16-silicon segments, with some emission occurring in competition, resulting in the same weak excitation energy dependence of the fluorescence shape.

In a high-viscosity medium, such as a low-temperature glass, the superficial nature of the near identity of the fluorescence properties of the high polymer and the hexadecasilane is revealed. Now, the absence of long-range energy transfer can no longer be compensated by conformational mobility, and the spectrum of the hexadecasilane changes dramatically.

Individual noncommunicating conformers now act independently, and three of them (A, B, and C) dominate the spectra. Their structures are not known, but they are clearly distinct from each other and from the presumably all-trans low-energy conformer or conformers that dominated room-temperature emission.

Even at concentrations as low as $5 \times 10^{-6}$ M, and more so at higher concentrations, $Si_{16}Me_{34}$ aggregates when its solution in 3-methylpentane is cooled rapidly to 77 K, and the picture is complicated further. The structure of the aggregate, termed dimer for simplicity, is not known, but it is likely to be a very loose, structurally disorganized collection of weakly communicating hexadecasilane molecules transferring energy to an emissive center that is probably similar to A.

Slow cooling and the use of higher concentrations results in the formation of microcrystals of a solid. Its absorption and emission properties fit expectations for a crystal that contains parallel chains of hexadecasilane molecules.

**Acknowledgment.** This work was supported by AFOSR Grant Nos. 87-0001, 89-0004, and 91-0032. We thank Dr. Robert D. Miller (IBM Almaden Research Center) for a kind gift of poly(methylpropylsilane) and Dr. Stephen J. Atherton for his help in the fluorescence lifetime measurements at the Center for Fast Kinetics Research, jointly supported by the Biotechnology Branch of the Division of Research Resources of the National Institutes of Health and the University of Texas at Austin.

# Photoreactivity of the Conjugate Bases of Two Aromatic Ketones: Photochemistry of the Enolates of $\alpha,\alpha$-Diphenylacetophenone and Deoxybenzoin

**Shiyamalie R. Ruberu and Marye Anne Fox***

*Contribution from the Department of Chemistry, University of Texas at Austin, Austin, Texas 78712.* *Received January 6, 1992*

**Abstract:** Photoexcitation of the enolate anion of deoxybenzoin (**4**) induces geomeric isomerization, as evidenced by ground state bleaching and formation of a metastable isomer. In aerated THF, the enolate of $\alpha,\alpha$-diphenylacetophenone **5** reacts by electron transfer to the excited triplet state of its thermal autoxidation product benzophenone. The calculated geometries of **4** and **5** (AM-1) correlate well with those found by solution and solid-state NMR spectroscopy, with enolate **4** existing as the more stable *Z*-isomer and enolate **5** in a twisted, locked geometry. The effect of ion pairing on the absorption spectra and the redox potentials of enolates **4** and **5** are discussed.

## Introduction

While it is well-known that photoexcitation of organic carbanions and oxyanions[1-3] often leads to different products than are formed from the excited states of their neutral precursors, the scope of such reactions and their applicability as efficient organic transformations have yet to be established. In particular, the structural features which cause the contrasting photoreactivity of neutral ketones and their conjugate base enolate anions[4-8] are unclear.

(1) Tolbert, L. M. *Acc. Chem. Res.* **1986**, *19*, 268.
(2) Tolbert, L. M. *Org. Photochem.* **1983**, *6*, 177.
(3) Fox, M. A. *Chem. Rev.* **1979**, *79*, 253.
(4) Scamehorn, R. G.; Bunnett, J. F. *J. Org. Chem.* **1977**, *42*, 1457.
(5) Rossi, R. A.; Bunnett, J. F. *J. Org. Chem.* **1973**, *38*, 1407.
(6) van Tamelen, E. E.; Schwartz, J.; Brauman, J. I. *J. Am. Chem. Soc.* **1970**, *92*, 5798.
(7) Padwa, A.; Dehm, D.; Oine, T.; Lee, G. A. *J. Am. Chem. Soc.* **1975**, *97*, 1837.
(8) Westmore, R. W.; Schaefer, H. F.; Hiberty, P. C.; Brauman, J. I. *J. Am. Chem. Soc.* **1980**, *102*, 5470.

0002-7863/92/1514-6310$03.00/0 